ANALYSIS OF CROSS SECTIONS AND ANALYZING POWERS IN THE p–He^3 ELASTIC SCATTERING USING A SPIN-DEPENDENT MODIFIED KRATZER POTENTIAL

P. Sahoo

Department of Physics, Dharanidhar University
Keonjhar, Odisha, 758001, India
nlphy.pati7@gmail.com

Received 12 April 2025, accepted 30 April 2026, published online 3 August 2026

This study explores the elastic scattering of charged hadronic system through a new approximation scheme for the effective potential. The Phase Function Method (PFM) is employed to examine the scattering phase shifts in the p–He^3 system, where a modified Kratzer potential is enhanced by electromagnetic interactions and spin–orbit coupling. A six-parameter potential model is developed and optimized to match the calculated scattering phase shifts, differential cross-sections, and proton analyzing power curves with experimental data for the p–He^3 system. The results show strong consistency with experimental measurements and previous theoretical predictions, affirming the accuracy and utility of the proposed method in analyzing scattering phenomena within this system.

DOI:10.5506/APhysPolB.57.9-A1

1. Introduction

The mechanism of nucleon–nucleus interactions is naturally complex because each projectile nucleon can easily interact with other nucleons within the nucleus. The microscopic model [1, 2] offers a comprehensive view of the interaction between the incoming nucleon and the nucleus, ensuring a more precise depiction of the fundamental physical processes. Qingbiao *et al.* [3] introduced the semi-microscopic nuclear matter method as an advanced technique for calculating the optical potential, utilizing the local density approximation to derive first- and second-order mass operators in asymmetric nuclear matter with Skyrme effective interactions. Studies conducted recently [1, 4, 5] have underscored the effectiveness of the phenomenological optical model potential in providing a more accurate analysis of nucleon–nucleus interactions. Koning *et al.* [6] introduced revised phenomenological optical model potential parameters, enabling the prediction of key scattering observables for spherical nuclides across a broad mass range and incoming energies from 1 KeV to 200 MeV. There is ambiguity regarding whether an equivalent calculation has been effectively extended to the four-nucleon (N–t) system, or if the theoretical framework is nearly finalized. Even within the separable potential model, achieving precise calculations remains challenging. It would be interesting to explore how a simpler approach might account for experimental observations. The strong nuclear interaction is still a major unresolved issue in the nuclear domain, despite extensive efforts in research. Much attention has been given to the three-nucleon system, with a focus on solving the N–d dispersion problem. Kamada *et al.* [7] approached the $4N$ bound state issue numerically, applying the AV18 nucleon–nucleon interaction to assess the binding energies and other system properties. By applying the Faddeev–Yakubovsky formalism, Lazauskas *et al.* [8] advanced the understanding of the N-body problem in non-relativistic quantum mechanics, providing successful explanations for the four- and five-nucleon systems using modern nuclear Hamiltonians. Watanabe *et al.* [9, 10] examined p–He^3 elastic scattering, studying spin correlation coefficients at both intermediate and high-energy levels, and found that the outcomes from different methods were in close agreement. More recently, comparable results were obtained when different $NN + 3N$ interactions were examined [11–14]. This research addresses the four-body scattering issue through the application of the Kohn variational principle and the use of hyperspherical (HH) functions to expand the core part of the wave function [15, 16]. This method, when applied with the local AV18 potential, was supported by Lazauskas *et al.* [8], Viviani *et al.* [17, 18], and Wiringa *et al.* [19], while non-local interactions are covered in Refs. [20–22]. References [23, 24] offer precise benchmark calculations for n+H^3 and p+He^3 elastic scattering and charge exchange processes, utilizing HH functions [23]. On the other hand, there is a lack of precise calculations for the p+H^3 and n+He^3 systems below the d–d threshold, with only a few studies yielding accurate results in this particular energy range [25–28]. Within this energy range, experimental data has been collected for the p+H^3 elastic differential cross section [29–33], the n+He^3 elastic cross section [34, 35] and total cross section [35, 36], as well as several n+He^3 elastic polarization observables [37–40].

For accurate evaluation of three-nucleon scattering observables, the Faddeev theory serves as a robust framework, with early studies relying on S-wave separable N–N potentials, whose parameters were fitted to match low-energy scattering results. However, including higher-order N–N partial-wave interactions in the calculations is essential for achieving a more precise understanding of spin observables. With advancements in N–N data, computational methods, and technology, more realistic N–N forces have-been developed, significantly improving the accuracy of three-nucleon calculations. To compute cross sections and analyzing power accurately, it is essential to determine the scattering phase shifts in each relevant partial wave state. The primary goal of this research is to determine phase parameters and related observables using the phase function method (PFM) [41–46], applied within the two-body interaction model that incorporates both nuclear and electromagnetic forces. For the nuclear interaction, the modified Kratzer potential [47–58] is adopted, and the Manning–Rosen potential [59–65] is used to simulate electromagnetic effects.

Researchers aim to improve magic number predictions by modifying nuclear models to better reflect real nuclear behavior. This includes more accurate modeling of potential energies, improved understanding of nucleon interactions, and the inclusion of effects such as deformation and pairing. Such refinements enhance our ability to describe the structure and stability of nuclei, especially for exotic and superheavy isotopes. Continued development of nuclear theory, alongside insights from experimental studies of rare nuclei, is critical for uncovering the nature of nuclear forces and structure. The idea of incorporating a spin–orbit potential to split nuclear subshells was successfully proposed by Mayer [66], Haxel [67], and their associates in 1949. Spin–orbit coupling, originally a concept from atomic physics, explains the fine structure of spectral lines through the interaction between an electron's magnetic moment and the magnetic field generated by its motion around the nucleus. Electromagnetic spin–orbit coupling has only a minor impact on atomic energy levels, roughly one part in 10^5, and cannot account for the larger energy gaps observed in nuclear spectra. For this reason, a corresponding spin–orbit term is incorporated into nuclear potential models. One-gluon exchange (OGE) [68] has been suggested as a potential origin of velocity-dependent forces such as spin–orbit coupling, a theory supported by strong polarization effects seen in nucleon–nucleus scattering and the evident doublet level splitting explained by the shell model. The exact dynamical source of the strong nuclear spin–orbit interaction remains unclear [69], although comparisons with atomic systems imply that it may have a relativistic origin. Experimental observations indicate that, at lower energies, nuclear interactions are largely governed by static, or velocity-independent, potentials. At higher energies, the forces are affected by the relative momentum $P = P_1 - P_2$ of the nucleons. Here, P_1 and P_2 denote the momenta of the individual nucleons, and according to Galilean invariance, the interaction depends only on their relative motion, not their absolute motion at any given moment during the interaction. Thus, for a two-body interaction, the only possible spin–orbit coupling is $V_{\mathrm{KRSO}}(r)((\vec{r} \times \vec{P}) \cdot \vec{S})$. In this case, $V_{\mathrm{KRSO}}(r)$

corresponds to the spin–orbit potential, which takes a form similar to the central potential but with different parameter. The variable r represents the relative distance between the nucleons during the interaction. This distinction highlights the unique nature of the spin–orbit interaction, which is governed by both the relative distance and the specific parameters of the potential. The expectation value of the spin–orbit interaction is directly proportional to $2\langle\vec{L}\cdot\vec{S}\rangle = J(J+1)-L(L+1)-S(S+1)$, where L, S, and J represent the orbital angular momentum, spin angular momentum, and total angular momentum, respectively. This proportionality highlights the dependence of the spin–orbit interaction on the combined contributions of orbital and spin angular momenta, influencing the system's overall behavior. Although the spin–orbit potential is typically considered a surface term and proportional to $\frac{1}{r}\frac{\mathrm{d}V}{\mathrm{d}r}$ [70], its influence is most pronounced at the nuclear surface, where the spin density is minimal inside the nucleus. However, we employ the modified Kratzer-like spin–orbit term [47–58], added with the central modified Kratzer potential, hypothesizing that it will take care of the varying effects of the interior and surface of the nucleus with suitable parameterization of the potential. It is also well known that the form of the potential in spin–orbit term $V_{\mathrm{KRSO}}(r)(\vec{L}\cdot\vec{S})$ is not that vital, but it is the $(\vec{L}\cdot\vec{S})$ factor which contributes significantly to reordering the levels. A significant spin–orbit coupling potential appears to be advantageous in explaining high-energy data.

The Kratzer potential [47–58] is a widely used model in nuclear and atomic physics to describe the interaction between two particles, typically nucleons or atoms. This potential, introduced by H. Kratzer in the early 20^{th} century, is an improvement over the simpler Coulomb or Lennard–Jones potentials, as it incorporates both attractive and repulsive forces with greater accuracy, particularly at short distances. The Kratzer potential is especially useful for modeling systems where the interaction between particles exhibits a more complex behavior, such as in molecular or nuclear binding. It is a type of repulsive potential that accounts for the nature of the short-range interactions between two particles, typically represented by a function that includes both an inverse distance term and a constant. Its application extends to various fields, including the study of vibrational spectra in molecules and the modeling of nuclear reactions. By providing a more realistic description of interparticle forces, the Kratzer potential helps in understanding the underlying mechanisms of particle interactions in both quantum and classical contexts. The incorporation of spin–orbit interaction into the Kratzer potential framework in this study is intended to enhance the precision of nucleon–nucleus interaction models, crucial for understanding nuclear structure. The Phase Function Method (PFM) [41–46] is applied to handle the angular dependencies and quantum mechanical properties of these interactions, ensuring a comprehensive approach to nuclear forces.

The Phase Function Method (PFM) has been utilized by several researchers to calculate quantum mechanical scattering phase shifts for different types of potentials [42–46, 71]. The pure Coulomb potential is an infinitely long-range interaction but in reality, it becomes screened at a certain distance. Thus, people prefer to use a screened or cut-off Coulomb interaction to deal with such situations within the framework of ordinary scattering theory. It is argued that the traditional PFM [41] does not hold good for pure Coulomb and Coulomb-like interactions and needs modification. As the Coulomb potential turns out to be insignificant after a finite distance, the use of the pure Coulomb interaction may be justified in many situations where scattering takes place under the combined influence of Coulomb-like potentials. Recently, Behera *et al.* [72] advocated that the use of the pure Coulomb or Coulomb-like potential in the traditional PFM is justified in many situations where the Coulomb potential is in fact always screened.

More recently, Behera *et al.* [73] investigated nucleon–nucleon and alpha–nucleon elastic scattering within the Manning–Rosen potential, while Sahoo *et al.* [46] focused on F- and G-partial wave nucleon–nucleon scattering using the Hulthén potential. Recent research [53–58] has extensively utilized the Kratzer potential to model molecular interactions and solve the Schrödinger equation in various contexts. Edet *et al.* [74] utilized the screened modified Kratzer potential within the non-relativistic regime, applying the Nikiforov–Uvarov Functional Analysis (NUFA) method to derive energy spectra and corresponding eigenfunctions. Ibrahim *et al.* [75] applied the extended Nikiforov–Uvarov method to solve the Schrödinger equation with the shifted screened Kratzer potential.

The methodology adopted in this work is briefly outlined in Section 2. Section 3 delivers an in-depth discussion of the results obtained, and Section 4 concludes by summarizing the major findings and their implications.

2. Methodology

The modified Kratzer potential [47–52] reads as

$$V_{\mathrm{KR}}(r) = V_0\left[1 - \frac{r_e}{r}\right]^2 ; \tag{1}$$

for $r_e = \frac{2}{\alpha}$,

$$V_{\mathrm{KR}}(r) = V_0\left[1 - \frac{2}{\alpha r}\right]^2 = V_0\left[1 + \frac{4}{\alpha^2 r^2} - \frac{4}{\alpha}\right] . \tag{2}$$

The effective modified Kratzer potential [47–52] is formulated in all partial waves as

$$V_{\mathrm{KRL}}(r) = V_0\left[1+\frac{4}{\alpha^2 r^2}-\frac{4}{\alpha}\right]+\frac{\ell(\ell+1)}{r^2}\,, \tag{3}$$

and the effective spin–orbit coupling is taken as

$$V_{\mathrm{KRSO}}(r) = V_1\left[1+\frac{4}{\alpha^2 r^2}-\frac{4}{\alpha}\right]\left(\vec{L}\cdot\vec{S}\right). \tag{4}$$

Here, α represents the inverse range parameter with units of fm^{-1}, while V_0 and V_1 are the strength parameters with units of fm^{-2}.

In order to study charged hadron systems, it is essential to include an electromagnetic interaction in addition to the nuclear potential. The Coulomb potential, in theory, permits an interaction over an infinite range. However, in reality, it is screened beyond a certain distance, making the Coulomb potential effectively negligible after a finite range. Driven by this consideration, the electromagnetic potential is modeled as a screened Manning–Rosen potential [59–63, 65, 76]

$$V_{\mathrm{M}}(r) = \frac{1}{b^2}\left[\beta(\beta-1)\frac{\exp\left(-2r/b\right)}{\left[1-\exp\left(-r/b\right)\right]^2}-A\frac{\exp\left(-r/b\right)}{\left[1-\exp\left(-r/b\right)\right]}\right]. \tag{5}$$

The parameters β and A are dimensionless parameters, while b represents the screening radius of the potential, with units of length. The effective equivalent potential under study for the charged hadron system is consequently

$$V(r) = V_{\mathrm{KRL}}(r)+V_{\mathrm{KRSO}}(r)+V_{\mathrm{M}}(r)\,. \tag{6}$$

The PFM [41–46] is an efficient computational approach that provides a strong substitute for the standard techniques used to solve the Schrödinger equation. Equation (4) is evaluated by implementing the standard prescription, the PFM to potential scattering [41]. The PFM offers an innovative prescription for calculating phase parameters in quantum mechanical problems, bypassing the need to solve the standard wave equation. The PFM operates by dividing the radial wave function of the Schrödinger equation into an amplitude factor $A_\ell(k,r)$ and an oscillating element with a variable phase $\delta_\ell(k,r)$. This means separating the two effects of the potential, which are manifested in the deformation of the wave function and the creation of the scattering phases [42, 71]. The function $\delta_\ell(k,r)$, called the phase function, at each point corresponds to the phase shift of the wave function when scattered by the potential truncated at a certain distance r. A potential that is fully cut off does not cause any phase shift. Therefore, the phase function is $\delta_\ell(k,r)=0$. The approach is based on transforming second-order linear homogeneous equations into first-order non-linear Riccati equations or phase equations, as demonstrated below

$$\delta'_\ell(k,r) = -k^{-1}V(r)\left[\cos\delta_\ell(k,r)\hat{j}_\ell(kr) - \sin\delta_\ell(k,r)\hat{\eta}_\ell(kr)\right]^2 , \tag{7}$$

where $\hat{j}_\ell(kr)$ and $\hat{\eta}_\ell(kr)$ are the Riccati–Bessel functions [77]. The resulting phase equations [41–46] for $\ell = 0, 1$ and 2 read as

$$\delta'_0(k,r) = -k^{-1}V(r)[\sin(\delta_0(k,r)+kr)]^2 , \tag{8}$$

$$\delta'_1(k,r) = -\frac{V(r)}{k^3r^2}[\sin(\delta_1(k,r)+kr) - kr\cos(\delta_1(k,r)+kr)]^2 , \tag{9}$$

and

$$\delta'_2(k,r) = -k^{-1}V(r)\left[\left(\frac{3}{k^2r^2}-1\right)\sin(\delta_2(k,r)+kr) - \frac{3}{kr}\cos(\delta_2(k,r)+kr)\right]^2 . \tag{10}$$

The parameter k is the center-of-mass momentum, and it is related to the center-of-mass energy through the equation $k = \sqrt{\frac{2mE}{\hbar^2}}$. The scattering phase shift $\delta_\ell(k,r)$ is calculated by solving the phase equation from the origin to the asymptotic region, given the initial condition $\delta_\ell(k,0) = 0$. During the solution of the phase equation $\delta_\ell(k,r)$, the value is gradually increased by the potential as one moves away from the origin, eventually reaching its asymptotic value once outside the range of the potential. Obviously, $\delta_\ell(k) = \lim_{r\to\infty}\delta_\ell(k,r)$. By knowing the phase function $\delta_\ell(k,r)$, the amplitude function $A_\ell(k,r)$ can be straightforwardly derived. Given the initial condition, the phase equations outlined in Eqs. (5)–(8) are solved numerically for the potential under investigation to match the scattering phase shifts, differential cross section, and proton analyzing power for the p–He^3 system.

3. Results and discussion

The computational model focuses on determining the elastic scattering phase shifts, differential cross section, and analyzing power for the p–He^3 interaction. In this context, $\hbar^2/2m$ is taken as 27.6467 MeV fm^2 for the system under consideration, where m denotes the reduced mass. To match the standard phase parameters for various states of the p–He^3 system, the nuclear modified Kratzer potential is parameterized, incorporating the spin–orbit term as given in Eqs. (4)–(6), and solved numerically through the differential equations (7)–(9). The parameters that best fit different angular momentum states of the system are presented in Table 1.

Using the scattering phase shift equation and the potential parameters provided above, the elastic scattering phase parameters for different states of the p–He^3 system are depicted in Figs. 1–3, together with the standard

Table 1. List of parameters for the p–He^3 system.

States	V_0	V_1	α	b	β	A
$^1S_0$	5.109	3.363	1.28	1.02	0.05	8.11
$^3S_1$	4.234	3.225	1.11	1.04	0.05	5.35
$^1P_1$	2.980	23.851	0.260	2.83	0.05	15.66
$^3P_0$	13.875	3.336	0.82	1.83	0.05	12.92
$^3P_1$	25.564	2.750	1.07	1.53	0.05	16.95
$^3P_2$	32.564	25.045	1.19	1.67	0.05	23.63

data from Daniels *et al.* [78]. Daniels *et al.* used a polarized He^3 target to measure the angular distributions of spin-correlation coefficients at proton energies between 2 and 6 MeV.

This new data was included in a global phase-shift analysis, building upon the work of George and Knutson [79] and also incorporating Fisher's data [80]. In a recent study, Viviani *et al.* [81] investigated several low-energy and charge-exchange reactions, including p–He^3 elastic reactions. They solved the four-body scattering problem using the Kohn variational principle and used hyper-spherical harmonic (HH) functions to expand the wave function's "core" part, which describes the interaction between closely bound particles. They observed that in p–He^3 scattering, both S- and P-wave phase shifts differed from experimental data when using only an NN potential. Adding the $3N$ force improved the agreement with phase-shift data. The elastic scattering of the p–He^3 system has been widely studied by various researchers [12, 13, 82–84]. This study examines p–He^3 elastic scattering through a simple central potential model using the phase-function technique, aiming to assess the model's ability to produce realistic results.

Figure 1 shows that the scattering phase shifts for the $^1S_0$ and $^3S_1$ states align well with the results reported by Daniels *et al.* [78]. However, the phase shift for the $^1S_0$ state shows a deviation of 2° to 3° in the high-energy region from the standard data, whereas those for the $^3S_1$ state closely follow the expected values, with a small deviation of around 1° at $E_{\mathrm{Lab}} = 2.25$ MeV. Looking at Fig. 2, it is evident that the scattering phase shifts for both the $^1P_1$ and $^3P_0$ states fall within the experimental error range [78], although the phase shift for the $^1P_1$ state shows a slightly larger deviation at higher energies. Figure 3 indicates that the results for the $^3P_1$ and $^3P_2$ states generally align with those of Daniels *et al.* [78], with slight deviations in phase shift at higher energies. Nevertheless, the analysis produces accurate phase shifts for most p–He^3 states, with minor discrepancies at higher energies possibly resulting from limitations of the potential model in capturing experimental force behavior. However, the variation remains within acceptable error margins and does not suggest significant flaws in the calculations.

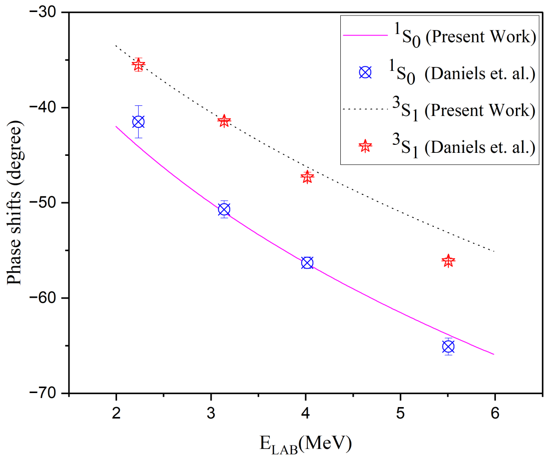

Fig. 1. Scattering phase shifts for the p–He^3 system in the ${}^1S_0$ and ${}^3S_1$ states as a function of lab energy are compared with standard values from Ref. [78].

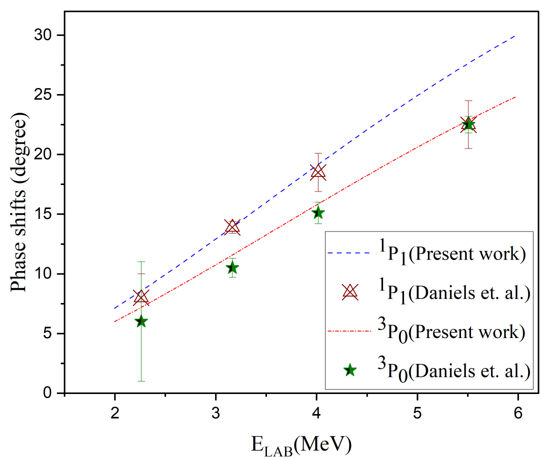

Fig. 2. Scattering phase shifts for the p–He^3 system in the ${}^1P_1$ and ${}^3P_0$ states as a function of lab energy are compared with standard values from Ref. [78].

Given the observable differences from existing phase-shift data, the study examines how the derived phase parameters reproduce cross-section data and proton analyzing power. The data in Figs. 4–9 illustrate the differential cross-section and proton analyzing power for the p–He^3 system, compared with reference results.

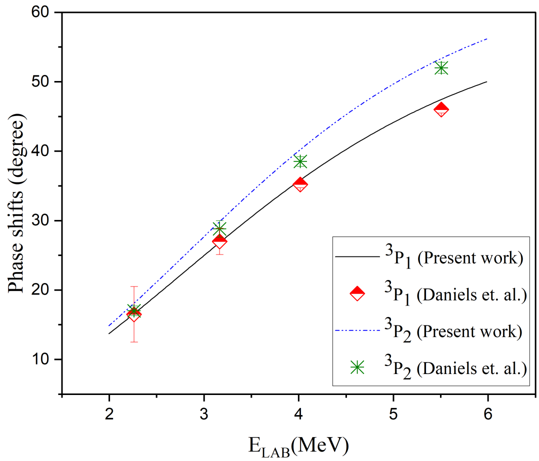

Fig. 3. Scattering phase shifts for the p–He^3 system in the $^3P_1$ and $^3P_2$ states as a function of lab energy are compared with standard values from Ref. [78].

Based on the extracted phase parameters, the model produces both the differential cross section and the corresponding proton analyzing power. In Figs. 4–6, the p–He^3 differential cross section is shown alongside previously available experimental and theoretical data for three distinct energies, $E_{\mathrm{Lab}} = 2.25$ MeV, 3.11 MeV, and 4.05 MeV demonstrating good agreement with Ref. [78]. As depicted in Fig. 4, the computed cross section at $E_{\mathrm{Lab}} = 2.25$ MeV aligns well with the findings of Viviani *et al.* [81] and Fisher *et al.* [80], despite minor differences at lower angles. In Fig. 5, the

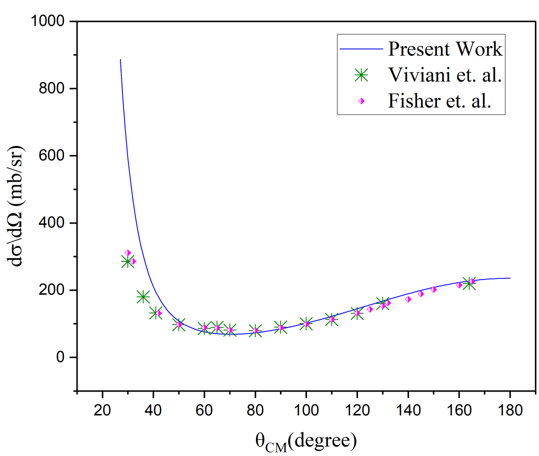

Fig. 4. p–He^3 differential cross section for $E_{\mathrm{Lab}} = 2.25$ MeV with standard data referenced from Refs. [80, 81].

differential scattering cross-section data for $E_{\mathrm{Lab}} = 3.11$ MeV correspond closely with the results of Fisher *et al.* [80]. The calculated cross-section points follow a similar progression to Ref. [80], with a small deviation observed at forward angles.

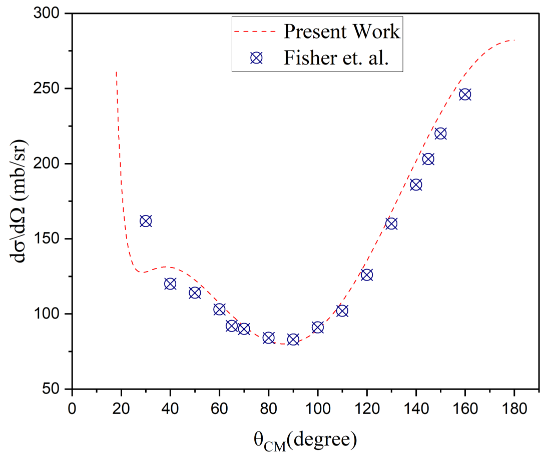

Fig. 5. p–He^3 differential cross section for $E_{\mathrm{Lab}} = 3.11$ MeV with standard data referenced from Refs. [80, 81].

Figure 6 shows that the differential cross section for a lab energy of 4.05 MeV is in excellent agreement with McDonald *et al.* [82] and Fisher *et al.* [80] from angles 70° to 165°, but there is a small deviation in the cross-section

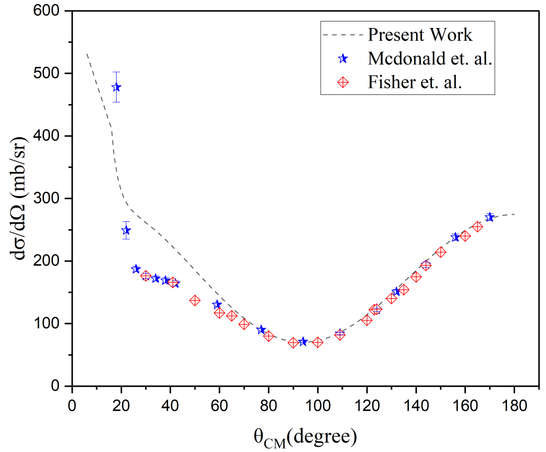

Fig. 6. p–He^3 differential cross section for $E_{\mathrm{Lab}} = 4.05$ MeV with standard data referenced from Refs. [80, 81].

values for angles less than 70°. The calculated minimum values of p–He^3 cross sections are 68.64, 80.02, and 70.04 mb/sr at $\theta_{\rm CM} = 70°, 86°$ and 94°, while those for Fisher *et al.* [80] are 80.24, 83, and 69.41 mb/sr at $\theta_{\rm CM} = 80°, 90°, 90°$ with the proton energies 2.25, 3.11, and 4.05 MeV, respectively. Viviani *et al.* [81] reported a minimum cross-section of 79 mb/sr at a center-of-mass angle of 80° for $E_{\rm Lab} = 2.25$ MeV, while McDonald *et al.* [82] measured a cross section of 71 mb/sr at 94° for proton energy of 4.05 MeV. The calculated minimum cross-section value coincides precisely with that of McDonald *et al.* [82] at a center-of-mass angle of 94°. Watanabe *et al.* [9, 10] reported substantial discrepancies in the region around the cross-section minimum when their results were compared with high-precision four-nucleon scattering calculations based on realistic nucleon–nucleon potentials. In general, the calculated cross sections are consistent with the trends observed in Refs. [80–82]. The minor deviation at forward angles could be attributed to slight variations in the scattering phase shift data, arising from the use of a screened Coulomb potential like the Kratzer potential. By examining analyzing power, one can gain insight into the spin-dependent aspects of the nuclear force and better understand the spin structure of the nucleus. In p–He^3 scattering, analyzing power indicates the preferential direction of scattered protons relative to the incoming proton beam and its defined plane. Proton analyzing power is a significant quantity measured in proton scattering experiments on nuclei. Although the model employs a simple central potential without tensor interactions, it still attempts to compute the proton analyzing power, as shown in Figs. 7–9. The calculated analyzing power shows a qualitative agreement with the results of Fisher *et al.* [80], although it is quantitatively lower than the data from Ref. [80] over a wide range of

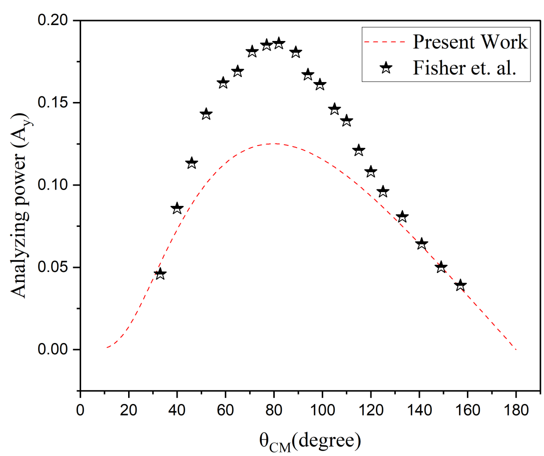

Fig. 7. The proton analyzing power for $E_{\rm Lab} = 2.25$ MeV is presented, with reference data taken from [80].

angles. However, the calculated results are consistent with the theoretical predictions for the AV18 and AV18/UIX potential models [17, 85], with the exception of large angles.

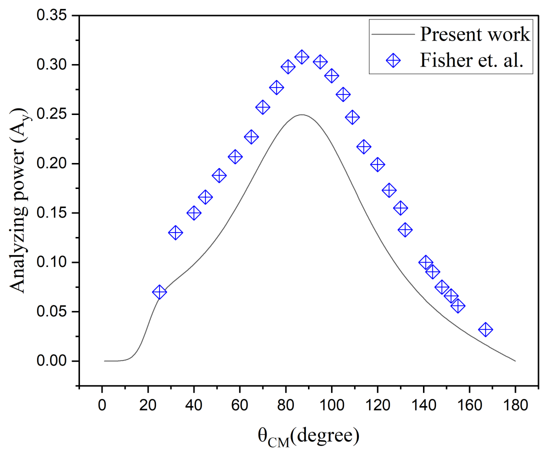

Fig. 8. The proton analyzing power for $E_{\mathrm{Lab}} = 3.11$ MeV is presented, with reference data taken from [80].

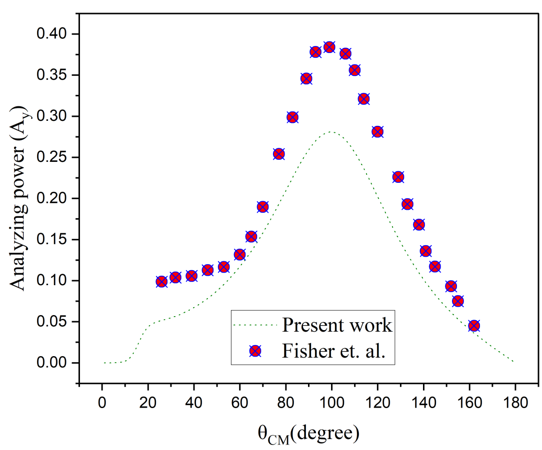

Fig. 9. The proton analyzing power for $E_{\mathrm{Lab}} = 4.05$ MeV is presented, with reference data taken from [80].

Although the analyzing power should reach zero at 180°, the calculated results show it tending toward zero with a very shallow gradient, yielding a value of about 0.05 at this angle. This difference is likely due to the use of a cross-section formula for a screened Coulomb potential instead of the pure Coulomb potential. Figures 10 and 11 display the potentials for all states up to $r = 3$ fm, highlighting the extended nature of the interaction. From the figures, it is clear that they exhibit similar behavior, decreasing with nearly identical gradients as the distance increases, due to the screened Coulomb-type interaction. Based on the results, the study demonstrates that the nuclear model achieves strong agreement with the observed phase shifts, cross sections, and analyzing power for the p–He^3 system.

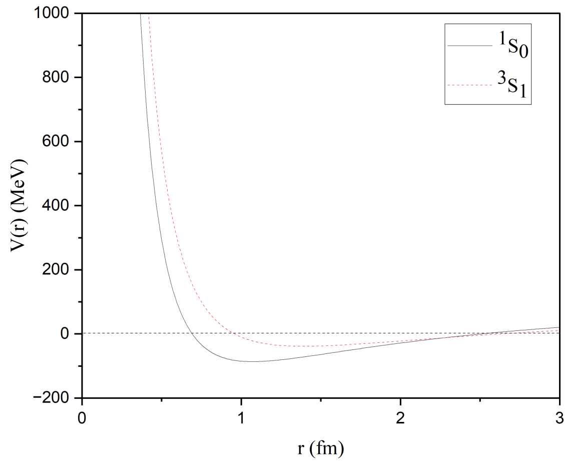

Fig. 10. The S-wave potentials for p–He^3 system are shown as a function of r.

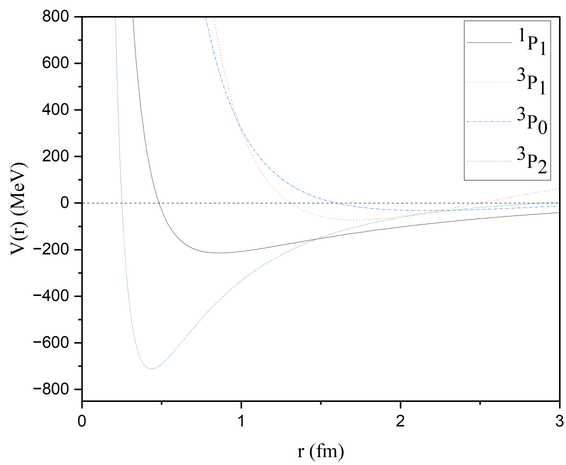

Fig. 11. The P-wave potentials for p–He^3 system are shown as a function of r.

4. Conclusions

This study employs the phase-function technique [41–46] alongside the modified Kratzer and Manning–Rosen potentials to investigate nucleon–nucleus elastic scattering, incorporating electromagnetic effects and evaluating the model's effectiveness through phase shifts, cross sections, and analyzing powers. The six-parameter potential model yields elastic scattering phase shifts for various p–He^3 states that are consistent with standard datasets [78]. Cross sections and analyzing powers were evaluated, incorporating the influence of the S- and P-waves. The calculated phase shifts, while differing numerically, still appropriately represent the respective states of the systems. The differences observed in the cross-section results, compared to both other theoretical studies and experimental data, are likely due to the small error margin in scattering phase shifts in the high-energy regime, which points to the likely lack of actual three-nucleon forces and may indicate the necessity of incorporating tensor interactions. Nevertheless, the model yields a satisfactory level of agreement with the experimental data. The analyzing power results align with experimental trends qualitatively but differ in magnitude, likely as a result of not including four-nucleon interactions. The present results for the analysing powers are in conformity with the observations of Viviani *et al.* [83] with AV18 potential and Swain *et al.* [86]. The investigation demonstrates that accurately modeling high-energy scattering demands a nuclear potential with dominant spin–orbit coupling at large radii and hard-core-like repulsion at short range. Motivated by the achievements of this study, future work aims to improve calculations by factoring in polarization effects for cases with unpolarized incident and target particles. Future research will focus on spin–orbit coupling, incorporating a second-order approximation for momentum. The current potential model may attract the interest of theoretical physicists, given the impressive consistency observed between theoretical and experimental results.

Data availability statement

The author declare that the data supporting the findings of this study are available within the paper.

REFERENCES

[1] M. Abusini, A. Ahbika, «Energy Sensitivity of the Low-energy Parameters of Neutron–Proton Scattering for Various Nucleon–Nucleon Potentials», *Rev. Cub. Fis.* **36**, 15 (2019).

[2] M.F. Alshudifat, M. Serhan, M. Abusini, «Elastic scattering of nucleon by the lightest mirror nuclei ^{3}H and ^{3}He using the optical model potential», *Int. J. Mod. Phys. E* **29**, 2050078 (2020).

[3] S. Qingbiao *et al.*, «Semi-microscopic optical potential calculation by the nuclear matter approach», *Z. Phys. A* **303**, 69 (1981).

[4] Q.-b. Shen, Y.-l. Han, H.-r. Guo, «Isospin dependent nucleon–nucleus optical potential with Skyrme interactions», *Phys. Rev. C* **80**, 024604 (2009).

[5] P.E. Hodgson, «The nuclear optical model introductory overview», Oxford Univ. Nucl. Phys. Tech. Rep., 1996, https://cds.cern.ch/record/317932

[6] A. Koning, J. Delaroche, «Local and global nucleon optical models from 1 keV to 200 MeV», *Nucl. Phys. A* **713**, 231 (2003).

[7] H. Kamada *et al.*, «Benchmark test calculation of a four-nucleon bound state», *Phys. Rev. C* **64**, 044001 (2001).

[8] R. Lazauskas, J. Carbonell, «Description of Four- and Five-Nucleon Systems by Solving Faddeev–Yakubovsky Equations in Configuration Space», *Front. Phys.* **7**, 251 (2020).

[9] A. Watanabe *et al.*, «Proton–^{3}He elastic scattering at intermediate energies», *Phys. Rev. C* **103**, 044001 (2021).

[10] A. Watanabe *et al.*, «Spin correlation coefficient for proton–^{3}He elastic scattering at 100 MeV», *Phys. Rev. C* **106**, 054002 (2022).

[11] A. Nogga *et al.*, «Three-nucleon bound states using realistic potential models», *Phys. Rev. C* **67**, 034004 (2003).

[12] R. Lazauskas, J. Carbonell, «Testing nonlocal nucleon–nucleon interactions in four-nucleon systems», *Phys. Rev. C* **70**, 044002 (2004).

[13] M. Viviani, A. Kievsky, S. Rosati, «Calculation of the α-particle ground state within the hyperspherical harmonic basis», *Phys. Rev. C* **71**, 024006 (2005).

[14] R.B. Wiringa, S.C. Pieper, J. Carlson, V.R. Pandharipande, «Quantum Monte Carlo calculations of $A = 8$ nuclei», *Phys. Rev. C* **62**, 014001 (2000).

[15] A. Kievsky *et al.*, «A high-precision variational approach to three- and four-nucleon bound and zero-energy scattering states», *J. Phys. G: Nucl. Part. Phys.* **35**, 063101 (2008).

[16] L.E. Marcucci *et al.*, «The hyperspherical harmonics method: a tool for testing and improving nuclear interaction models», arXiv:1912.09751 [nucl-th].

[17] M. Viviani *et al.*, «The A_y Problem for p–^{3}He Elastic Scattering», *Phys. Rev. Lett.* **86**, 3739 (2001).

[18] M. Viviani, S. Rosati, A. Kievsky, «Neutron–^{3}H and Proton–^{3}He Zero Energy Scattering», *Phys. Rev. Lett.* **81**, 1580 (1998).

[19] R.B. Wiringa, V.G.J. Stoks, R. Schiavilla, «Accurate nucleon–nucleon potential with charge-independence breaking», *Phys. Rev. C* **51**, 38 (1995).

[20] M. Viviani *et al.*, «Variational Calculation on $A = 3$ and 4 Nuclei with Non-Local Potentials», *Few-Body Syst.* **39**, 159 (2006).

[21] L.E. Marcucci *et al.*, «N–d elastic scattering using the hyperspherical harmonics approach with realistic local and nonlocal interactions», *Phys. Rev. C* **80**, 034003 (2009).

[22] M. Viviani *et al.*, «Neutron–Triton Elastic Scattering», *Few-Body Syst.* **45**, 119 (2009).

[23] M. Viviani *et al.*, «Benchmark calculation of n–^{3}H, p–^{3}He scattering», *Phys. Rev. C* **84**, 054010 (2011).

[24] M. Viviani *et al.*, «Benchmark calculation of p–^{3}H, n–^{3}He scattering», *Phys. Rev. C* **95**, 034003 (2017).

[25] A. Deltuva, A.C. Fonseca, «Four-nucleon scattering: *Ab initio* calculations in momentum space», *Phys. Rev. C* **75**, 014005 (2007).

[26] A. Deltuva, A. Fonseca, P. Sauer, «Four-nucleon system with Δ-isobar excitation», *Phys. Lett. B* **660**, 471 (2008).

[27] A. Deltuva, A. C. Fonseca, «Four-body calculation of elastic deuteron–deuteron scattering», *Phys. Rev. C* **92**, 024001 (2015).

[28] P. Sahoo, «Evaluation of n–p and n–d Analyzing Powers Through the Jost Formalism», *Braz. J. Phys.* **54**, 23 (2023).

[29] A. Hemmendinger, G. Jarvis, R. Taschek, «Scattering of Protons by Tritons», *Phys. Rev.* **76**, 1137 (1949).

[30] R.S. Claassen, R.J.S. Brown, G.D. Freier, W.R. Stratton, «The Scattering of Protons by Tritons», *Phys. Rev.* **82**, 589 (1951).

[31] M. Ivanovich, P. Young, G. Ohlsen, «Elastic scattering of several hydrogen and helium isotopes from tritium», *Nucl. Phys. A* **110**, 441 (1968).

[32] R. Kankowsky *et al.*, «Elastic scattering of polarized protons on tritons between 4 and 12 MeV», *Nucl. Phys. A* **263**, 29 (1976).

[33] N. Jarmie, R.C. Allen, «T(p,p)T Scattering Near the T(p,n)He^3 Threshold», *Phys. Rev.* **114**, 176 (1959).

[34] J.D. Seagrave, L. Cranberg, J.E. Simmons, «Elastic Scattering of Fast Neutrons by Tritium and He^3», *Phys. Rev.* **119**, 1981 (1960).

[35] A.R. Sayres, K. Jones, C. Wu, «Interaction of Neutrons with He^3», *Phys. Rev.* **122**, 1853 (1961).

[36] B. Haesner *et al.*, «Measurement of the ^{3}He and ^{4}He total neutron cross sections up to 40 MeV», *Phys. Rev. C* **28**, 995 (1983).

[37] C.E. Hollandsworth, M. Gilpatrick, W.P. Bucher, «Scattering of Polarized 3-MeV Neutrons from ^{3}He», *Phys. Rev. C* **5**, 395 (1972).

[38] H. Klages *et al.*, «Analyzing power of the n–^{3}He elastic scattering from 3.7 to 22.0 MeV», *Nucl. Phys. A* **443**, 237 (1985).

[39] P. Jany *et al.*, «Analyzing power of n–^{3}He elastic scattering from 1 to 2 MeV», *Nucl. Phys. A* **483**, 269 (1988).

[40] J. Esterline *et al.*, «Analyzing Power $A_y(\theta)$ n–^{3}He Elastic Scattering Between 1.60 and 5.54 MeV», *Phys. Rev. Lett.* **110**, 152503 (2013).

[41] F. Calogero, «Variable Phase Approach to Potential Scattering», Mathematics in Science and Engineering, Vol. 35, *Academic Press*, New York 1967.

[42] G.C. Sett, U. Laha, B. Talukdar, «Phase-function method for Coulomb-distorted nuclear scattering», *J. Phys. A: Math. Gen.* **21**, 3643 (1988).

[43] B. Swain, U. Laha, P. Sahoo, and A. Behera, «Phase function method for Hulthén-distorted separable non-local potentials in all partial waves», *Pramana* **96**, 162 (2022).

[44] B. Swain, U. Laha, A.K. Behera, «Low and intermediate energy cross section analysis of p–p and p–d elastic scattering using modified phase amplitude method for electromagnetic distorted nuclear interaction», *Phys. Scr.* **98**, 105308 (2023).

[45] P. Sahoo, U. Laha, «Phase shift and cross section analysis of nucleon–nucleon and nucleon–nucleus scattering using second Pöschl–Teller potential», *Can. J. Phys.* **101**, 441 (2023).

[46] U. Laha, P. Sahoo, A.K. Behera, B. Khirali, «Nuclear Hulthén Potentials for F and G Partial Waves», *Res. Rev.: J. Phys.* **10**, 31 (2021).

[47] A. Kratzer, «Die ultraroten Rotationsspektren der Halogenwasserstoffe», *Z. Physik* **3**, 289 (1920).

[48] D. Bouaziz, «Kratzer's molecular potential in quantum mechanics with a generalized uncertainty principle», *Ann. Phys.* **355**, 269 (2015).

[49] M.R. Setare, E. Karimi, «Algebraic approach to the Kratzer potential», *Phys. Scr.* **75**, 90 (2006).

[50] D. Bonatsos *et al.*, «Bohr Hamiltonian with a deformation-dependent mass term for the Kratzer potential», *Phys. Rev. C* **88**, 034316 (2013).

[51] N. Saad, R. Hall, H. Ciftci, «The Klein–Gordon equation with the Kratzer potential in d dimensions», *Open Phys.* **6**, 717 (2008).

[52] V. Kumar *et al.*, «Optical properties of spherical quantum dot using screened Kratzer potential», *Phys. B Condens. Matter* **683**, 415920 (2024).

[53] S.B. Doma, A.A. Gohar, M.S. Younes, «Analytical Solutions of the Molecular Kratzer–Feus potential by means of the Nikiforov–Uvarov Method», *J. Math. Chem.* **61**, 1301 (2023).

[54] A. Maireche, «Improved energy spectra of the deformed Klein–Gordon and Schrödinger equations under the improved Varshni plus modified Kratzer potential model in the 3D-ERQM and 3D-ENRQM symmetries», *Indian J. Phys.* **97**, 3567 (2023).

[55] A.N. Ikot *et al.*, «Klein–Gordon Equation and Nonrelativistic Thermodynamic Properties with Improved Screened Kratzer Potential», *J. Low Temp. Phys.* **202**, 269 (2021).

[56] R.Y. Kezerashvili, J. Luo, C.R. Malvino, «Bound state solutions of the two-dimensional Schrödinger equation with Kratzer-type potentials», `arXiv:2311.02694 [quant-ph]`.

[57] E.P. Inyang, E. Omugbe, M. Abu-shady, E.S. William, «Investigation of quantum information theory with the screened modified Kratzer and a class of Yukawa potential model», *Eur. Phys. J. Plus* **138**, 969 (2023).

[58] E.P. Inyang *et al.*, «Approximate solutions of the Schrödinger equation with Hulthén plus screened Kratzer Potential using the Nikiforov–Uvarov — functional analysis (NUFA) method: an application to diatomic molecules», *Can. J. Phys.* **100**, 463 (2022).

[59] P. Sahoo, U. Laha, «Exact solutions of the Schrödinger equation for Manning–Rosen plus Yamaguchi potential», *Phys. Scr.* **96**, 095302 (2021).

[60] P. Sahoo, U. Laha, «Nucleon–nucleus inelastic scattering by Manning–Rosen distorted nonlocal potential», *Can. J. Phys.* **100**, 68 (2022).

[61] B. Khirali, U. Laha, P. Sahoo, «Analytic transition matrix for the Manning–Rosen potential in all partial waves», *Chinese J. Phys.* **77**, 2355 (2022).

[62] P. Sahoo, U. Laha, B. Khirali, «Studies in scattering using Manning–Rosen-modified separable potential in all partial waves», *Pramana* **96**, 201 (2022).

[63] P. Sarkar, B. Khirali, U. Laha, P. Sahoo, «Exact solution of two-potential system under same range approximation and its implication», *Int. J. Mod. Phys. E* **30**, 215066 (2021).

[64] G.-F. Wei, C.-Y. Long, S.-H. Dong, «The scattering of the Manning–Rosen potential with centrifugal term», *Phys. Lett. A* **372**, 2592 (2008).

[65] G.-F. Wei, S.-H. Dong, «Pseudospin symmetry in the relativistic Manning–Rosen potential including a Pekeris-type approximation to the pseudo-centrifugal term», *Phys. Lett. B* **686**, 288 (2010).

[66] M.G. Mayer, «On Closed Shells in Nuclei. II», *Phys. Rev.* **75**, 1969 (1949).

[67] O. Haxel, J.H.D. Jensen, H.E. Suess, «On the "Magic Numbers" in Nuclear Structure», *Phys. Rev.* **75**, 1766 (1949).

[68] H. Hong-Xia *et al.*, «Influence of Spin–Orbit Force on Nucleon–Nucleon Scattering in the Quark Delocalization Colour Screening Model», *Chin. Phys. Lett.* **25**, 1617 (2008).

[69] N. Kaiser, «Nuclear spin–orbit interaction from chiral pion–nucleon dynamics», *Nucl. Phys. A* **709**, 251 (2002).

[70] M. Sajedi, Z. Kargar, «Shifted Deng–Fan potential and cluster structure in ^{19}Ne», *Nucl. Phys. A* **1015**, 122314 (2021).

[71] B. Talukdar, D. Chattarji, P. Banerjee, «A generalized approach to the phase-amplitude method», *J. Phys. G: Nucl. Phys.* **3**, 813 (1977).

[72] A.K. Behera, U. Laha, «Phase equivalent Coulomb-like potential», *Pramana* **95**, 103 (2021).

[73] A.K. Behera, J. Bhoi, U. Laha, B. Khirali, «Study of nucleon–nucleon and alpha–nucleon elastic scattering by the Manning–Rosen potential», *Commun. Theor. Phys.* **72**, 075301 (2020).

[74] C.O. Edet *et al.*, «Eigenfunctions, uncertainties and thermal properties of diatomic molecules under screened modified Kratzer potential», *Indian J. Phys.* **96**, 3429 (2022).

[75] N. Ibrahim *et al.*, «Solutions of the Schrödinger equation of the shifted screened Kratzer potential and its thermodynamic functions using the extended Nikiforov–Uvarov method», *Front. Phys.* **10**, 988279 (2022).

[76] P. Sahoo, U. Laha, «Treatment of hadronic systems involving two potentials under a new approximation scheme», *Pramana* **96**, 15 (2022).

[77] G.N. Watson, «A Treatise on the Theory of Bessel Functions», *The University Press*, 1922.

[78] T.V. Daniels *et al.*, «Spin-correlation coefficients and phase-shift analysis for $p+^3$He elastic scattering», *Phys. Rev. C* **82**, 034002 (2010).

[79] E. George, L. Knutson, «Scattering lengths for p–^{3}He elastic scattering from an effective-range phase shift analysis», *Phys. Rev. C* **67**, 027001 (2003).

[80] B. Fisher *et al.*, «Proton–^{3}He elastic scattering at low energies», *Phys. Rev. C* **74**, 034001 (2006).

[81] M. Viviani, L. Girlanda, A. Kievsky, L. Marcucci, «$n+^3$H, $p+^3$He, $p+^3$H, and $n+^3$He scattering with the hyperspherical harmonic method», *Phys. Rev. C* **102**, 034007 (2020).

[82] D.G. McDonald, W. Haeberli, L.W. Morrow, «Polarization and Cross Section of Protons Scattered by He^3 from 4 to 13 MeV», *Phys. Rev.* **133**, B1178 (1964).

[83] M. Viviani, L. Girlanda, A. Kievsky, L.E. Marcucci, «Recent Progress in *Ab-initio* Four-Body Scattering Calculations», *Few-Body Syst.* **54**, 647 (2012).

[84] Y. Yoshino *et al.*, «Phase Shifts of p–^{3}He Scattering at Low Energies», *Prog. Theor. Phys.* **103**, 107 (2000).

[85] B.S. Pudliner *et al.*, «Quantum Monte Carlo calculations of nuclei with $a \leq 7$», *Phys. Rev. C* **56**, 1720 (1997).

[86] B. Swain, D. Naik, U. Laha, «Cross-section analysis and analyzing power for p–^{3}He system via modified phase-amplitude method», *Eur. Phys. J. Plus* **140**, 127 (2025).